Search for production of an $\Upsilon(1S)$ meson in association with a W or Z boson using the full 1.96 TeV $p\bar{p}$ collision dataset at CDF

The CDF Collaboration

Abstract

Production of the $\Upsilon(1S)$ meson in association with a vector boson is a rare process in the standard model with a cross section predicted to be below the sensitivity of the Tevatron. Observation of this process could signify problems with the current non-relativistic quantum chromodynamics models used to calculate the cross section or contributions from physics beyond the standard model. We perform a search for this process using the full Run II dataset collected by the CDF II detector corresponding to an integrated luminosity of $9.4\,\mathrm{fb}^{-1}$. The search considers the $\Upsilon \to \mu\mu$ decay and the charged lepton decay modes of the W and Z bosons. In these purely leptonic decay channels, we observe one $\Upsilon + W$ candidate with an expected background of 1.2 ± 0.5 events, and one $\Upsilon + Z$ candidate with an expected background of 0.1 ± 0.1 events. Both observations are consistent with the predicted background contributions. We set the most stringent upper limits from a single experiment on the cross section for $\Upsilon + W/Z$ production, which also restricts potential contributions from non standard model physics.

PACS numbers: 14.70.-e, 4.40.Pq, 12.39.Jh

I. INTRODUCTION

The standard model production of an upsilon meson (Υ) in association with a W boson or a Z boson is a rare process that was first calculated in Ref. [1], where ΥW and ΥZ production occur through the parton level processes producing $W + b\bar{b}$ and $Z + b\bar{b}$ final states, in which the $b\bar{b}$ pair may form a bound state (either an Υ or an excited bottomonium state that decays to an Υ). More recently these processes have been calculated at next-to-leading-order in the strong-interaction coupling for proton-antiproton ($p\bar{p}$) collisions at 1.96 TeV center-of-mass energy and proton-proton collisions at 8 TeV and 14 TeV [2] .

The cross sections calculated for ΥW and ΥZ production in $p\bar{p}$ collisions at a center-of-mass energy of 1.96 TeV are 43 fb and 34 fb, respectively. These values were calculated at leading-order using the MadOnia quarkonium generator [3] as detailed below and are roughly a factor of 10 smaller than the earlier calculations from Ref. [1]. The calculations of these processes are very sensitive to the non-relativistic quantum chromodynamics (NRQCD) models, especially the numerical values of the long-distance matrix elements (LDME), which determine the probability that a $b\bar{b}$ will form a bottomonium state. Measurements of $\Upsilon + W/Z$ cross sections are important for validating these NRQCD models.

Supersymmetry (SUSY) is an extension of the standard-model (SM) which is yet to be experimentally observed. Reference [1] describes some SUSY models in which charged Higgs bosons can decay into ΥW final states with a large branching fraction (B). Similarly, in addition to the expected decays of a SM Higgs to an ΥZ pair, further light neutral scalars may decay into ΥZ. Therefore, if the observed rate of ΥW and/or ΥZ production is significantly larger than the predicted SM rate, it may be an indication of physics beyond the SM.

In 2003, the CDF collaboration reported [4] a search for the associated production of an upsilon meson and a W or Z boson. In that analysis, a sample corresponding to 83 pb^{-1} of 1.8 TeV $p\bar{p}$ collision data collected with the Run I CDF detector was used to set upper limits on the production cross sections at the 95% confidence level (CL) of $\sigma(p\bar{p} \to \Upsilon + W) \times \mathcal{B}(\Upsilon \to \mu^+\mu^-) < 2.3$ pb and $\sigma(p\bar{p} \to \Upsilon + Z) \times \mathcal{B}(\Upsilon \to \mu^+\mu^-) < 2.5$ pb.

Here we present a search for $\Upsilon + W/Z$ production, using a sample corresponding to 9.4 fb^{-1} of 1.96 TeV $p\bar{p}$ collision data collected with the CDF II detector. We use the dimuon decay channel to identify the upsilon meson. We use only the electron and muon decay channels

of the W and Z bosons, which give the best sensitivities for this search.

II. THE CDF DETECTOR

The CDF II detector is a nearly azimuthally and forward-backward symmetric detector designed to study $p\bar{p}$ collisions at the Tevatron. It is described in detail in Ref. [5]. It consists of a magnetic spectrometer surrounded by calorimeters and a muon-detection system. Particle trajectories are expressed in a cylindrical coordinate system, with the z axis along the proton beam and the x axis pointing outward from the center of the Tevatron. The azimuthal angle (ϕ) is defined with respect to the x direction. The polar angle (θ) is measured with respect to the z direction, and the pseudorapidity (η) is defined as $\eta = -\ln(\tan\frac{\theta}{2})$. The momentum of charged particles is measured by the tracking system, consisting of silicon strip detectors surrounded by an open-cell drift chamber, all immersed in a 1.4 T solenoidal magnetic field. The tracking system provides charged-particle trajectory (track) information with good efficiency in the range $|\eta| \lesssim 1.0$. The tracking system is surrounded by pointing-geometry tower calorimeters, which measure the energies of electrons, photons, and jets of hadronic particles. The electromagnetic calorimeters consist of scintillating tile and lead absorber, while the hadronic calorimeters are composed of scintillating tiles with steel absorber. The calorimeters comprise central and plug subdetectors, with the central region covering $|\eta| < 1.1$ and the plug region covering the range $1.1 < |\eta| < 3.6$. The muon system is composed of planar multi-wire drift chambers. In the central region, four layers of chambers located just outside the calorimeter cover the region $|\eta| < 0.6$. An additional 60 cm of iron shielding surrounds this system, and behind that is a second subdetector composed of another four layers of chambers. A third muon subdetector covers the region $0.6 < |\eta| < 1.0$, and a fourth subdetector extends coverage to $|\eta| < 1.5$. Cherenkov luminosity counters measure the rate of inelastic collisions, which is converted into the instantaneous luminosity. A three-level online event-selection system (trigger) is used to reduce the event rate from 2.5 MHz to approximately 100 Hz. The first level consists of specialized hardware, while the second is a mixture of hardware and fast software algorithms. The software-based third-level trigger has access to a similar set of information to that available in the offline reconstruction.

III. MONTE CARLO AND DATA SAMPLES

The analysis uses high-p_T lepton data sets, containing triggered events with a reconstructed electron or muon candidate of E_T (or p_T in the case of muon candidates) greater than 18 GeV (GeV/c). The integrated luminosity of these samples is 9.4 fb^{-1}. All the search channels include the $\Upsilon \to \mu\mu$ signal, so we only use data acquired when the muon detectors were operational, resulting in the same integrated luminosity for the electron and muon samples. We also use a low-p_T dimuon-triggered Υ sample for cross-checks and estimating backgrounds. The dimuon invariant-mass distribution from this low-p_T sample, whose integrated luminosity is 7.3 fb^{-1}, is shown in Fig. 1 for the mass range in the region of the upsilon resonances.

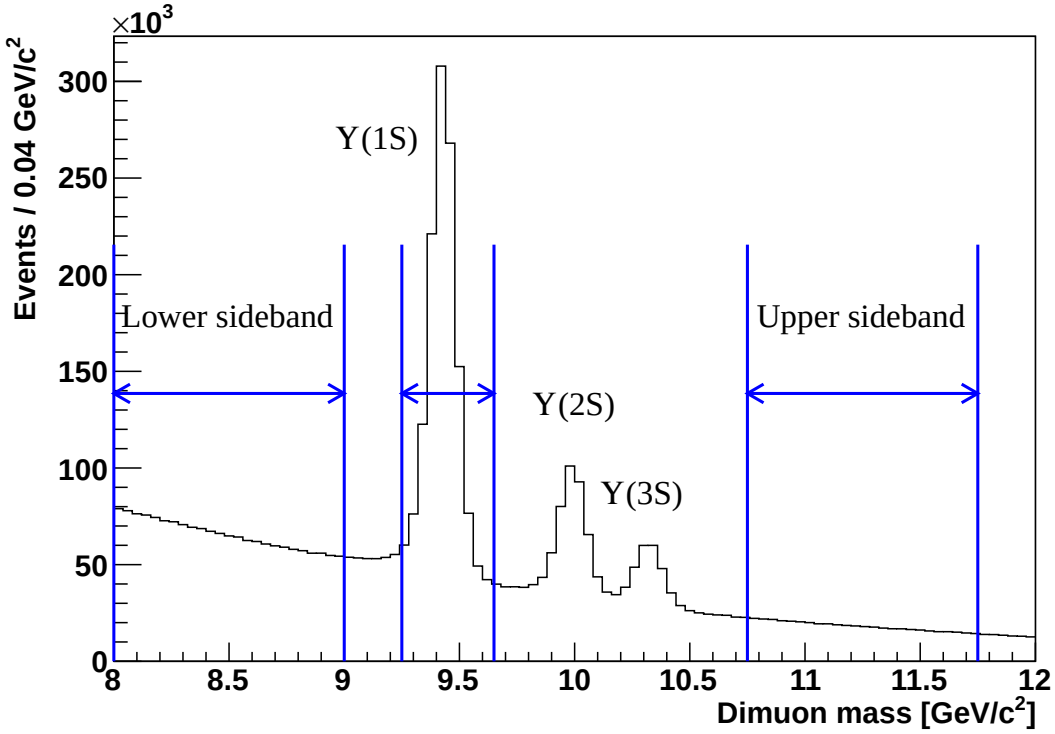

FIG. 1: Dimuon invariant-mass spectrum in CDF II data from events contained within the low-p_T dimuon-triggered sample. Shown is the defined Υ signal region and the sideband regions used for background determination.

We produce simulated event samples of the signal processes, ΥW and ΥZ, by first generating events with MadGraph [6] and its quarkonium extension MadOnia [3]. We include all ΥW and ΥZ processes from Ref. [1] and the LDME values relevant for the Tevatron

from Ref. [7]. The LDME values come from fits to quarkonia data. An explanation of how this is done is given in Ref. [8], although the values obtained in this reference are relevant for the LHC, not the Tevatron. PYTHIA [9] is used to simulate the Υ, W, and Z decays and parton showering. Generated upsilon mesons are forced to decay to two muons. We use a GEANT3-based [10] detector simulation to model the response of the CDF II detector [11].

IV. EVENT SELECTION

This analysis selects events with Υ mesons decaying to muon pairs and decays of vector bosons resulting in at least one electron or muon. We first select $\Upsilon(1S)$ candidates using the Υ decay to two low-p_T muons. We then look for additional high-energy electron (or muon) candidates indicative of a vector-boson decay. Events with exactly one high-energy lepton candidate, ℓ, which will henceforth refer to an electron or muon, in addition to the $\Upsilon \to \mu^+\mu^-$ candidate, and significant missing energy are selected as $\Upsilon + (W \to \ell\nu)$ candidates. Events with two oppositely charged high-energy lepton candidates of same flavor are selected as $\Upsilon + (Z \to \ell^+\ell^-)$ candidates. In the small fraction of events (less than 2%) that have more than two low-p_T muons identified we randomly choose one pair of those muons.

Before detailing the event-selection criteria, we define some quantities used in event selection. The transverse momentum of a charged particle is $p_T = p\sin\theta$, where p is the momentum of the charged particle track. The analogous quantity measured with the calorimeter is transverse energy, $E_T = E\sin\theta$. The missing transverse energy, $\not\!\!E_T$ is defined as $\vec{\not\!\!E}_T = -\sum_i E_T^i \hat{n}_i$, where $\hat{n}_i$ is a unit vector perpendicular to the beam axis and pointing to the center of the ith calorimeter tower. The $\vec{\not\!\!E}_T$ is adjusted for high-energy muons, which deposit only a small fraction of their energies in the calorimeter, and offline corrections applied to the measured energies of reconstructed jets [12]. We define $\not\!\!E_T = |\vec{\not\!\!E}_T|$. The invariant mass of two leptons is $M_{\ell\ell} = \sqrt{(E_{\ell 1} + E_{\ell 2})^2/c^4 - |\vec{p}_{\ell 1} + \vec{p}_{\ell 2}|^2/c^2}$, and the transverse mass of a lepton and neutrino (as measured by the $\not\!\!E_T$) is $M_T = \sqrt{2p_T^\ell \not\!\!E_T(1-\cos\phi)/c^3}$ where ϕ is the angle between the lepton track and $\not\!\!E_T$ vector in the transverse plane.

We define the upsilon(1S) region as the invariant-mass range $9.25 < M_{\mu\mu} < 9.65\,\mathrm{GeV}/c^2$. We do not use the upsilon 2S or 3S states in this analysis. We define two sideband regions, $8.00 < M_{\mu\mu} < 9.00\,\mathrm{GeV}/c^2$ and $10.75 < M_{\mu\mu} < 11.75\,\mathrm{GeV}/c^2$, for obtaining background estimates.

In this analysis we have two categories of lepton candidates: low-p_T muon candidates from the Υ decay and high-E_T(or p_T) electron (or muon) candidates from the W or Z decay. The high-$E_T(p_T)$ lepton candidate selection requires $E_T(p_T) > 15\,\mathrm{GeV}\,(\mathrm{GeV}/c)$ along with additional measurement and fiducial-volume quality criteria described in Ref. [13].

Events are required to have at least two low-p_T muon candidates with $1.5 < p_T < 15\,\mathrm{GeV}/c$, whose invariant mass lies within the upsilon(1S) region. To increase the upsilon-reconstruction efficiency, we use looser quality requirements on these low-p_T muon candidates than for the high-$E_T(p_T)$ vector-boson lepton candidates. In particular, there are no isolation requirements on the upsilon muon candidates, and matching requirements between reconstructed charged tracks and reconstructed track stubs in the muon detectors are less stringent.

From events containing a $\Upsilon \to \mu\mu$ candidate, we select $\Upsilon + (W \to \ell\nu)$ candidates by requiring exactly one additional electron (muon) candidate with E_T (p_T) greater than $20\,\mathrm{GeV}\,(\mathrm{GeV}/c)$. The electron or muon candidate is required to be isolated from other calorimeter activity such that additional calorimeter energies observed in a cone of $\Delta R = \sqrt{\Delta\eta^2 + \Delta\phi^2} = 0.4$ around the lepton candidate sum to no more than 10% of the electron candidate's energy or muon candidate's momentum. Additionally, we require that the event has $\not\!\!E_T > 20\,\mathrm{GeV}$ and transverse mass in the range $50 < M_T < 90\,\mathrm{GeV}/c^2$, as expected from a W boson decay. Figures 2 show the distributions of these quantities as predicted from the simulated $\Upsilon + W$ event samples.

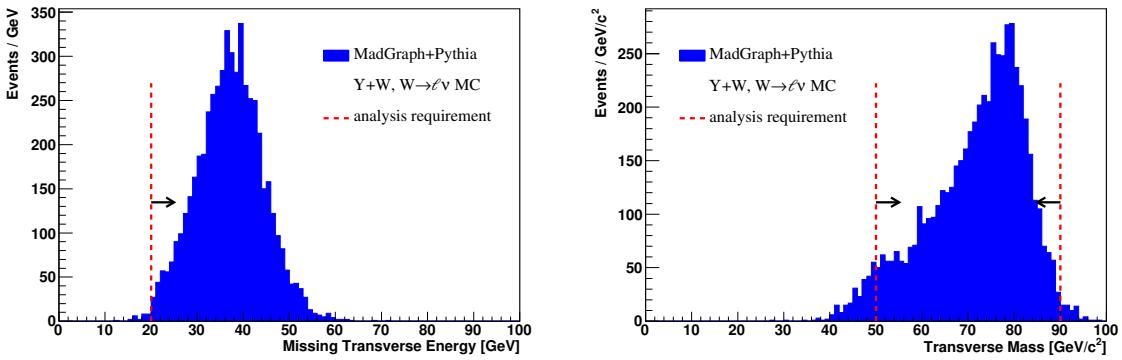

(a) (b)

FIG. 2: Missing-transverse-energy (a) and transverse-mass (b) distribution predicted for signal ΥW, $W \to \ell\nu$ events. The distribution is shown for events that satisfy all other event requirements. The scale of the vertical axis is arbitrary.

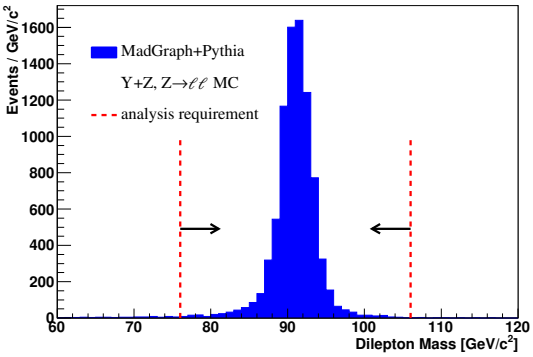

FIG. 3: Dilepton invariant-mass distribution predicted for signal ΥZ, $Z \to \ell\ell$ events. The distribution is shown for events that satisfy all other event requirements. The scale of the vertical axis is arbitrary.

The $\Upsilon + (Z \to \ell\ell)$ candidates are selected by requiring one additional high-$E_T(p_T)$ electron (muon) candidate with $E_T(p_T) > 20\,\mathrm{GeV}\,(\mathrm{GeV}/c)$ and a second candidate with the same flavor but opposite charge and $E_T(p_T) > 15\,\mathrm{GeV}\,(\mathrm{GeV}/c)$. Both additional lepton candidates are required to be isolated and have an invariant mass in the range $76 < M_{\ell\ell} < 106\,\mathrm{GeV}/c^2$. The invariant-mass distribution predicted from the simulated $\Upsilon + (Z \to \ell\ell)$ event samples is shown in Fig. 3.

The total signal efficiencies, after all selection criteria are applied, are determined from simulated event samples to be 1.8% for $\Upsilon + (W \to e\nu)$, 1.3% for $\Upsilon + (W \to \mu\nu)$, 1.8% for $\Upsilon + (Z \to ee)$, and 1.4% for $\Upsilon + (Z \to \mu\mu)$ events. These efficiencies do not include the branching fractions for $\Upsilon \to \mu\mu$ and the electronic and muonic decays of the vector bosons. The low acceptances are primarily driven by the geometric acceptance of the drift chamber for the two low-p_T muons from the upsilon decay. We expect a small contribution to the $W \to \ell\nu$ acceptance from $W \to \tau\nu$ events where the tau lepton decays to an electron or muon. The contribution is determined to be less than 2% of the acceptance, and is therefore neglected. The contribution from $Z \to \tau\tau$ events to the $Z \to \ell\ell$ channels is also determined to be negligible.

Summaries of the selection criteria and their associated efficiencies are given in Tables I and II.

TABLE I: Efficiencies for the $(\Upsilon \to \mu\mu) + (W \to \ell\nu)$ selection criteria. The listed acceptance values correspond to efficiencies for each of the listed requirements subsequent to the application of the previously listed criteria. Sources to the uncertainty quoted on the total efficiency are discussed in the text.

	$\Upsilon + W \to e\nu$	$\Upsilon + W \to \mu\nu$
$\Upsilon(1S) \to \mu\mu$ candidate	6.8%	6.8%
One additional high-$E_T(p_T)$ isolated e or μ candidate	55%	46%
High-$E_T(p_T)$ lepton candidate is triggerable	55%	52%
$\not\!\!E_T > 20\,\mathrm{GeV}$	96%	94%
$50 < M_T < 90\,\mathrm{GeV}/c^2$	94%	95%
Trigger efficiency	97%	92%
Total	$(1.8 \pm 0.4)\%$	$(1.3 \pm 0.3)\%$

TABLE II: Efficiencies for the $(\Upsilon \to \mu\mu) + (Z \to \ell\ell)$ selection criteria. The listed acceptance values correspond to efficiencies for each of the listed requirements subsequent to the application of the previously listed criteria. Sources to the uncertainty quoted on the total efficiency are discussed in the text. OS means opposite-sign.

	$\Upsilon + Z \to ee$	$\Upsilon + Z \to \mu\mu$
$\Upsilon(1S) \to \mu\mu$ candidate	6.7%	7.0%
Two additional OS high-$E_T(p_T)$ isolated e or μ candidates	32%	25%
One of the two high-$E_T(p_T)$ lepton candidates is triggerable	86%	80%
$76 < M_{\ell\ell} < 106\,\mathrm{GeV}/c^2$	99%	99%
Trigger efficiency	98%	95%
Total	$(1.8 \pm 0.4)\%$	$(1.4 \pm 0.3)\%$

V. BACKGROUNDS

There are two main background contributions to the signal samples: events containing a correctly identified W/Z candidate and a misidentified upsilon candidate (real W/Z + fake upsilon) and those with a correctly identified upsilon candidate and a misidentified W/Z candidate (real upsilon + fake W/Z). Generic dimuon backgrounds, originating predominantly from $b\bar{b}$ production, contribute events in the invariant-mass range defined for the Υ(1S) and are the primary source of fake upsilon candidates. Misidentification of parton jets as leptons can mimic the decay signatures of W and Z bosons. In the case of Z candidates, where two leptons are required, this background is estimated to be negligible.

The real W/Z + fake upsilon background contributions are estimated by counting the

number of W or Z candidate events in the high-p_T lepton data samples that additionally contain a dimuon candidate in the sideband region of the dimuon spectrum (defined in Fig. 1). An exponential fit to these sideband regions is used to determine a ratio of the areas of the signal to sideband regions, which is then applied to these numbers for an estimate of this background contribution.

The probabilities for reconstructed jets to be misidentified as leptons are measured in data as functions of the jet E_T and lepton type using the procedure described in Ref. [13]. To estimate real upsilon + fake W/Z background contributions, we select from the low-p_T dimuon data sample events containing a high-E_T jet instead of a high-E_T (p_T) isolated lepton candidate that otherwise satisfy the full selection criteria. Background estimates are obtained using the measured probabilities associated with each of the jets within these events as weighting factors on the potential contribution of each. The low-p_T dimuon sample is relied upon to extract these background estimates because a strong correlation between high-p_T lepton trigger selection requirements and jet-to-lepton misidentification rates renders the high-p_T lepton data set unsuitable for the chosen methodology. To extrapolate between the two samples, additional small correction factors are applied to account for differences in the integrated luminosites of the two samples and upsilon selection inefficiencies in the low-p_T dimuon sample originating from trigger requirements.

The predicted background contributions to each of the signal samples are summarized in Table IV. In evaluating the real Z + fake upsilon background contribution, no events containing upsilon candidates in the sideband mass regions are observed. Background contributions to the corresponding signal samples are therefore estimated by extrapolating from the estimated real W + fake upsilon background contributions, using the ratio of Z-to-W cross sections, under the assumption that the fake upsilon probability is independent of the type of vector boson. In calculating cross-section limits, we also account for small background contributions from ΥZ production to the ΥW samples originating from events in which one of the two leptons produced in the Z boson decay is not reconstructed.

VI. SYSTEMATIC UNCERTAINTIES

For determining cross-section limits on the targeted processes, we incorporate systematic uncertainties on the signal expectation and the background predictions.

Systematic uncertainties on the signal expectation include those associated with the integrated luminosity measurement, low-p_T muon identification, high-$E_T(p_T)$ lepton identification, high-$E_T(p_T)$ lepton trigger efficiency, theoretical modelling of the signal, and efficiencies of the event selection criteria. The upsilon-muon identification uncertainty is taken from Ref. [14], while the high-$E_T(p_T)$ lepton identification and trigger efficiency uncertainties are derived from Ref. [13].

We use the CTEQ6L parton distribution functions (PDFs) for generating the MadGraph samples. To estimate the acceptance uncertainty associated with the choice of PDFs, we generate additional samples using MRST PDFs and take the difference in the estimated signal acceptance as the uncertainty.

We vary the bottomonium LDMEs by one standard deviation to estimate their effect on the signal acceptance, where both the nominal values and uncertainties are from Ref. [7]. This procedure results in an additional 6% systematic uncertainty on the signal acceptance. These uncertainties only account for those associated with the procedure for computing LDMEs described within this particular reference and that different assumptions used in the fits for calculating LDMEs can lead to a wider range of results. We do not attempt to account for differences in LDMEs resulting from different fits. However, if an arbitrarily chosen uncertainty of 20% were to be placed on the LDMEs, the cross-section limits we obtain would only increase by about 10%.

With respect to uncertainties associated with event selection criteria, we vary the $\not\!\!E_T$ by $\pm 10\%$ (an estimate of the $\not\!\!E_T$ resolution) in the simulated signal samples to quantify the effect of $\not\!\!E_T$ resolution.

It is possible for the Υ meson and the W or Z boson to originate from different parton-parton interactions in the same $p\bar{p}$ collision. This double-parton-scattering process is difficult to identify, but estimates have been made for several related final states using LHC and Tevatron data (see for example Refs. [**?**]). These estimates together with a calculation using the Υ and vector boson cross sections at $\sqrt{s} = 2\,\text{TeV}$ lead to an estimated effect of roughly 15%. Based on our lack of knowledge of this effect we assign this effect as a systematic uncertainty on the signal acceptance. Systematic uncertainties associated with the signal expectation are summarized in Table III.

Uncertainties on predicted background contributions are also incorporated into the cross-section limits. For the real W/Z + fake upsilon background, we use the statistical uncer-

tainty originating from the small sample size in the sideband regions used for making this estimate. We assign a 50% uncertainty to the real upsilon + fake W/Z background based on the application of uncertainties associated with the measured jet-to-lepton misidentification rates.

TABLE III: Systematic uncertainties associated with the signal expectation.

Luminosity	6%
Upsilon muon identification	4%
High-$E_T(p_T)$ lepton identification	1%
High-$E_T(p_T)$ lepton trigger efficiency	1%
PDFs	12%
LDMEs	6%
Double parton scattering	15%
Event selection efficiency	3%
Total	22%

VII. RESULTS

Table IV summarizes the predicted signal and background contributions, and number of observed events for each of the targeted search samples using $9.4\,\mathrm{fb}^{-1}$ of CDF Run II data. We observe one $\Upsilon + (W \to \ell\nu)$ candidate with a total expected background of 1.2 ± 0.5 events and one $\Upsilon + (Z \to \ell\ell)$ candidate with a total expected background of 0.1 ± 0.1 events. An event display of the $\Upsilon + (Z \to \ell\ell)$ candidate is shown in Fig. 4. This is the first observed $\Upsilon + (Z \to \ell\ell)$ candidate event. The two high-p_T muon candidates have an invariant mass of $88.6\,\mathrm{GeV}/c^2$, and the two low-p_T muon candidates have an invariant mass of $9.26\,\mathrm{GeV}/c^2$. All muon candidates are detected in the central region of the detector. The invariant mass of all four muon candidates is $98.4\,\mathrm{GeV}/c^2$.

Having observed no clear evidence for a $\Upsilon + W/Z$ signal, we set 95% confidence level (C.L.) upper limits on the ΥW and ΥZ production cross sections. In calculating these limits we use the branching fractions of $\Upsilon \to \mu\mu$ (0.0248), $W \to \ell\nu$ (0.107), and $Z \to \ell\ell$ (0.0336) from Ref. [17]. A Bayesian technique [15] was employed, where the posterior probability density was constructed from the joint Poisson probability of observing the data in each vector boson decay channel, integrating over the uncertainties of the normalization parameters using Gaussian priors. A non-negative constant prior in the signal rate was assumed. The

TABLE IV: Summary of signal expectation (N_{sig}), background estimations (N_{bg}), and observed events (N_{obs}) for each of the targeted search samples using $9.4\,\mathrm{fb}^{-1}$ of CDF II data.

	$\Upsilon + W \to e\nu$	$\Upsilon + W \to \mu\nu$	$\Upsilon + W \to \ell\nu$	$\Upsilon + Z \to ee$	$\Upsilon + Z \to \mu\mu$	$\Upsilon + Z \to \ell\ell$
N_{sig}	0.019±0.004	0.014±0.003	0.034±0.007	0.0048±0.0011	0.0037±0.0008	0.0084±0.0018
N_{bg} (fake Υ)	0.7±0.4	0.4±0.3	1.1±0.5	0.07±0.07	0.04±0.04	0.1±0.1
N_{bg} (fake W/Z)	0.06±0.04	0	0.06±0.04	0	0	0
N_{bg} ($\Upsilon + Z$)	0.0006±0.0001	0.0033±0.0007	0.0039±0.0009			
N_{bg} (total)	0.8±0.4	0.4±0.3	1.2±0.5	0.07±0.07	0.04±0.04	0.1±0.1
N_{obs}	0	1	1	0	1	1

expected and observed limits are shown in Table V and compared to the observed limits from the CDF Run I analysis [4].

TABLE V: Cross-section limits at 95% C.L. for ΥW and ΥZ production. This analysis utilizes $9.4\,\mathrm{fb}^{-1}$ of CDF II Run II data. The Run I analysis utilized $83\,\mathrm{pb}^{-1}$ of CDF Run I data.

	$\Upsilon + W$	$\Upsilon + Z$
Expected limit (pb)	5.6	13
Observed limit (pb)	5.6	21
Run I observed limit (pb)	93	101

VIII. CONCLUSIONS

We search for $\Upsilon + W/Z$ production using the leptonic decay channels of the vector bosons and dimuon decay channel of the upsilon. The search utilizes the full CDF Run II data set. Having observed no significant excess of events, we set 95% C.L. upper limits on the $\Upsilon + W/Z$ cross sections, which are the best limits to date on these processes. Since it is not expected that potential non-SM physics contributions to the $\Upsilon + W/Z$ final state significantly impact the kinematic properties of events, these limits can be interpreted as cross section (times branching ratio to $\Upsilon + W/Z$) limits on non-SM physics process contributing to this final state. Potential new heavy particles decaying to $\Upsilon + W/Z$ final states may likely tend to produce leptons that are more central than those from standard-model $\Upsilon + W/Z$ production and therefore might result in higher signal acceptance. Hence, the limits presented here can be considered as upper limits on such processes.

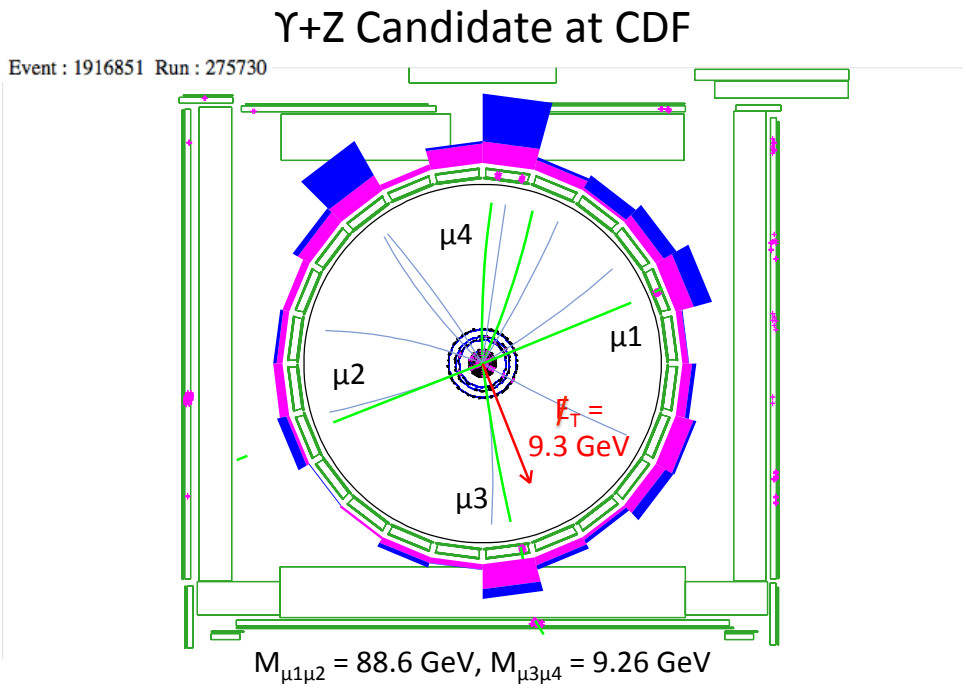

FIG. 4: Event display of the observed $\Upsilon + Z$ candidate, showing the muon candidates identified from the Υ and Z decays.

IX. ACKNOWLEDGMENTS

We would like to acknowledge K. W. Lai for suggesting the search for these processes, and thank P. Artoisenet and J.-P. Lansberg for many useful discussions and help with theoretical inputs into the MadGraph simulation.

We thank the Fermilab staff and the technical staffs of the participating institutions for their vital contributions. This work was supported by the U.S. Department of Energy and National Science Foundation; the Italian Istituto Nazionale di Fisica Nucleare; the Ministry of Education, Culture, Sports, Science and Technology of Japan; the Natural Sciences and Engineering Research Council of Canada; the National Science Council of the Republic of China; the Swiss National Science Foundation; the A.P. Sloan Foundation; the Bundesministerium für Bildung und Forschung, Germany; the Korean World Class University Program, the National Research Foundation of Korea; the Science and Technology Facilities Council and the Royal Society, United Kingdom; the Russian Foundation for Basic Research; the Ministerio de Ciencia e Innovación, and Programa Consolider-Ingenio 2010, Spain; the Slovak R&D Agency; the Academy of Finland; the Australian Research Council (ARC); and

the EU community Marie Curie Fellowship Contract No. 302103.

---

[1] E. Braaten, J. Lee and S. Fleming, Phys. Rev. D **60**, 091501 (1999).

[2] B. Gong, J. -P. Lansberg, C. Lorce and J. Wang, J. High Energy Phys. **03**, 115 (2013).

[3] P. Artoisenet, F. Maltoni and T. Stelzer, J. High Energy Phys. **02**, 102 (2008).

[4] D. Acosta *et al.* [CDF Collaboration], Phys. Rev. Lett. **90**, 221803 (2003).

[5] F. Abe *et al.* [CDF Collaboration], Nucl. Instrum. Meth. A **271**, 387 (1988); D. E. Amidei *et al.* [CDF Collaboration], Nucl. Instrum. Meth. A **350**, 73 (1994); F. Abe *et al.* [CDF Collaboration], Phys. Rev. D **52**, 4784 (1995); S. Cihangir, G. Gillespie, H. Gonzalez, S. Gonzalez, C. Grimm, M. Guerra, T. Hawke and M. Hrycyk *et al.*, Nucl. Instrum. Meth. A **360**, 137 (1995); R. Blair *et al.* [CDF Collaboration], FERMILAB-DESIGN-1996-01.

[6] J. Alwall, P. Demin, S. de Visscher, R. Frederix, M. Herquet, F. Maltoni, T. Plehn and D. L. Rainwater *et al.*, J. High Energy Phys. **09**, 028 (2007).

[7] E. Braaten, S. Fleming and A. K. Leibovich, Phys. Rev. D **63**, 094006 (2001).

[8] R. Sharma and I. Vitev, Phys. Rev. C **87**, 044905 (2013).

[9] T. Sjostrand, S. Mrenna and P. Z. Skands, J. High Energy Phys. **05**, 026 (2006).

[10] R. Brun, F. Carminati and S. Giani, CERN-W5013.

[11] E. Gerchtein and M. Paulini, eConf C **0303241**, TUMT005 (2003).

[12] D. Acosta *et al.* [CDF Collaboration], Nucl. Instrum. Meth. A **461**, 540 (2001).

[13] T. Aaltonen *et al.* [CDF Collaboration], Phys. Rev. D **88**, no. 5, 052012 (2013).

[14] T. Aaltonen *et al.* [CDF Collaboration], Phys. Rev. Lett. **108**, 151802 (2012).

[15] Junk, T.. Sensitivity, Exclusion and Discovery with Small Signals, Large Backgrounds, and Large Systematic Uncertainties. - (2007). CDF/DOC/STATISTICS/PUBLIC/8128.

[16] [ATLAS Collaboration], ATLAS-CONF-2013-042.

[17] J. Beringer *et al.* [Particle Data Group Collaboration], Phys. Rev. D **86**, 010001 (2012).